Zero Energy Visible Light Communication Receiver for Embedded Applications

Prabhakar T V
Indian Institute of Science
Bangalore, India
tvprabs@dese.iisc.ernet.in

Vishwas Shashidhar*, G S Aishwarya Meghana
NITK, Surathkal
Mangalore, India
*vishwas.shashidhar.79@gmail.com

R. Venkatesha Prasad
Delft University of Technology
Delft, The Netherlands
r.r.venkateshaprasad@tudelft.nl

Garani Vittal Pranavendra
Indian Institute of Technology
Bhubaneswar, India
pg13@iitbbs.ac.in

ABSTRACT

Internet of Things is bringing multiple domains and multiple avenues to connect anything and everything. It mainly uses RF connectivity. However, recently visible light communication (VLC) is also being explored. VLC has the properties that are unique with respect to the privacy and security that it provides. Though the transmission is of broadcast in nature the receiver needs to be in the vicinity of the transmitter, thus providing secure communications. Further, when low power receivers need to be constructed, it is important to harness energy from transmission itself. In this article we propose a novel design for a receiver to be used in VLC for embedded systems. The setup works, using a small solar panel (2mm x 2mm) as a medium to simultaneously harvest incident light energy and receive data bit streams. The LED source was modulated using On-Off Keying. The receiver works for close range communications. The results in this paper show experimental evaluation of the system. We could detect the signals from the source using harvested energy from the same transmission.

KEYWORDS

Visible light communication, Energy Harvesting, Photovoltaic Cell, LED, Receiver, High Pass Filter, Peak Detector, Nano-Power Comparator

ACM Reference Format:
Prabhakar T V, Vishwas Shashidhar*, G S Aishwarya Meghana, R. Venkatesha Prasad, and Garani Vittal Pranavendra. 2017. Zero Energy Visible Light Communication Receiver for Embedded Applications. In *Proceedings of Advances in IoT Architecture and Systems, Toronto, Canada, June 2017 (AIoTAS'17)*, 7 pages.

1 INTRODUCTION

While several spectral efficiency mechanisms attempt to improve the spectrum usage of present day cellular networks, there continues to be a constant shortage in spectrum availability due to the proliferation of IoT devices. Optical Wireless Communication in the Infra-Red and visible light regions is the best solution to meet the increasing requirements for bandwidth by users. The visible light spectrum is 10,000 times larger than RF spectrum. In particular, this spectrum is found to be attractive in line of sight and close proximity communication between source and destination. Further, these systems cause no electromagnetic interference (EMI), thus allowing access to communicate in locations where RF communication is restricted and sometimes infeasible. [1–4]

Compared to RF technology, VLC is highly energy efficient, as illumination and data transmission are done simultaneously. The data sent by a VLC transmitter is received by a VLC receiver with a typical distance of a few centimetres. This finds application in several scenarios. For instance, untethered localized communication might be required in assembly and production environments. Drug concentration levels can be programmed for a batch. Similar examples can be envisaged for fortification. Here, a dosifier dispenses a premix to a beverage to obtain the necessary nutrients personalized for a patient. A light source from the dispenser powers the transceiver that contains information of the premix. This data is relayed back to the dosifier. Accordingly, the system actuators on the dosifier dispense the premix.

A conventional VLC system consists of a commercially available LED as a transmitter. The receiver is typically a photodiode in reverse bias. These systems rely on the light's amplitude to encode data as the actual phase of the light cannot be changed. The simplest of them all is On-Off Keying, where the rapid blinking of an LED is exploited to transmit a 1 (on) or a 0 (off). This is detected by the photodiode and communication is established. Since the eye perceives sources blinking above 60Hz to be constant sources, there is no strain on the retina due to VLC. Such a receiver system, however, demands external power supply. In our proposed system, we use a miniature solar panel as the VLC receiver as well as an energy harvester. There are many applications for such harvest & communication systems. While the dual purpose is a welcome measure since it helps in miniaturization of receivers. For example, an air Marshall on a plane could be contacted directly using his reading light, which is highly secure and no others could snoop the transmission since it is almost a directed light source (and transmission). The system we propose here has lowest form factor of (2 mm x 2 mm) solar cell and a board of size (6 mm x 10 mm); thus it could be hidden in a wearable device.

This paper deals with the building of such a miniaturized VLC system with harvesting. We provide complete design and experimental results of such a system in this article. We propose a zero

AIoTAS'17, June 2017, Toronto, Canada

energy VLC receiver that can interpret the data and harvest energy from the received data using a photovoltaic panel. We provide the characteristics, system and measurements with respect to the datarate that could be achieved. In the following sections, we describe the characterization of the panel and the design of the energy harvesting receiver circuit. The paper also lists some experiments which were carried out to assess the performance of the receiver.

2 RELATED WORKS

The efficiency of solar cell is continuously increasing by the efforts of many researchers [5]. This implies that for a solar panel of a given size, the power harvested is significantly high. Hence small and miniature solar panels can power dense circuits. Due to the awareness and usage of green technology in all domains, solar cells are widely being used in many devices to generate electrical energy from the external incident light. Recent studies have shown solar cells are versatile for communication, being used as broadband receivers [6]. With the growing efficiency of solar cells, small panels can support large data rates. The work done by Sung-Man Kim et al. [7], proposes a VLC system which uses the solar cell to receive data and harvest energy from the sunlight. They have successfully demonstrated that stable communication is possible even in the presence of interference of sunlight without loss of information.

The work reported in Joice Sariol Ramos et.al [8] is mainly used to generate a wake up call for a mote class device. The wake-up receiver has an energy harvesting circuit for powering an OOK demodulator and for recognition of the node ID. Since there is no data transmission, the circuit has limitations with respect to achievable data rates.

A novel LED based energy harvesting system is proposed by Xiaozhe Fan et. al [9]. However, the control circuitry to place the LEDs in harvesting region consumes significant power.

In the work reported by Bilal Malik et. al [10], the authors propose a signal conditioning unit to shape the output from the solar panel. However, there is no mention of the circuit and the duration over which the system can sustain when the input data stream contains continuous 0s. The results have been reported for 50% duty cycle square waves.

2.1 DC Characterization of the Solar Cell

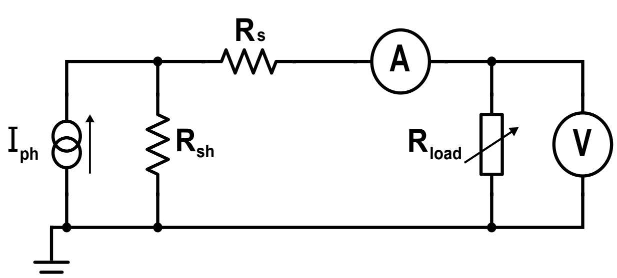

Figure 1: Equivalent DC model of the solar panel

The DC model of a photovoltaic cell, shown in Fig 1 has been studied and well established in [11–13]. The voltage and current of the solar panel have a nonlinear relationship. This is modelled by a diode connected in parallel to photocurrent I_{ph}. The voltage loss due to cell interconnections, is modelled by a series resistor R_s and the leakage current is modelled by a shunt resistor R_{sh}. Using the above equivalent circuit, the I-V characteristics of the panel is obtained as,

$$I = I_{ph} - I_D - \frac{V + IR_s}{R_{sh}} \tag{1}$$

where V is the voltage seen across the load resistor and I_D is the current through the diode. From semiconductor physics, this current is given by

$$I_D = I_0 exp(\frac{V + IR_s}{\eta V_T}) \tag{2}$$

where I_0 is the reverse saturation current of the diode, η is the diode ideality factor, and V_T is the thermal voltage that is taken to be 0.0257 V in our calculations.

A simple I-V characteristic experiment was performed by noting the voltage V and current I at various loads. A potentiometer was used for changing the load. Following this procedure, an optimization algorithm was used as described in [13] to estimate the values of η , R_s and R_{sh}. The algorithm follows a regression method to estimate the parameters. It utilizes the measured values of I and V to optimize a theoretical current I_{th}, which is given by :

$$I_{th} = \frac{V_{oc} - V_{exp} - I_{exp}.R_s}{R_{sh}} - \frac{[I_{sc}(1 + \frac{R_s}{R_{sh}}) - \frac{V_{oc}}{R_s h}].(exp(-\frac{V_{oc}-V_{exp}-I_{exp}.R_s}{\eta V_T}) - 1)}{1 - exp(\frac{I_{sc}.R_s - V_{oc}}{\eta V_T})} \tag{3}$$

The objective function is constructed to minimize the error between the theoretical and experimental values of current.

$$J = |I_{exp} - I_{th}|^2 \tag{4}$$

The results for the two panels is summarized in Table 1. The I-V and P-V curves of the panels at their respective intensities are shown in Fig. 2 and Fig. 3.

Table 1: Results of DC Characterization

Panel	CPC1824	SP4.2-37
Intensity (LUX)	3000	6150
R_{sh} in $M\Omega$	83.7	102.3
R_s in Ω	1.69	0.069

2.2 Frequency Response of the Solar Panel

In order to read intensity modulated data, the solar panel must be capable of producing similar alternating voltages at the same frequency as the input. This calls for the AC modeling of the panel which analyses its performance for communication purposes.

The AC equivalent circuit of the panel is obtained by modifying the equivalent circuit of Fig.1. The diode is replaced by its small-signal equivalent resistor r, and a capacitor C is introduced parallel to R_{sh} to account for the internal capacitive effects of the panel. It is important to note here that irrespective of the input, the panel

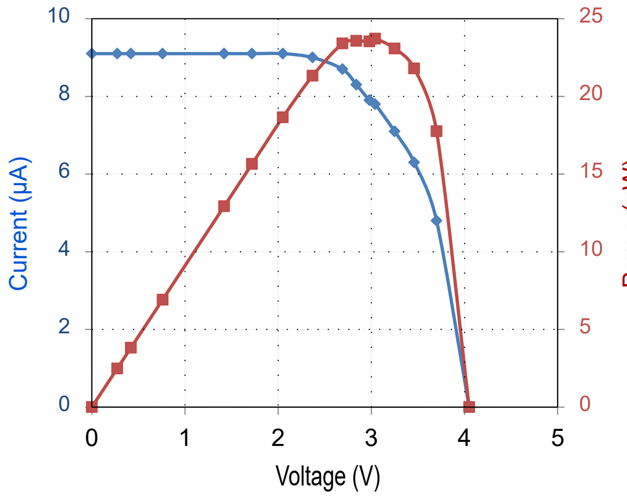

Figure 2: DC Characteristics of CPC1824 at 3000LUX

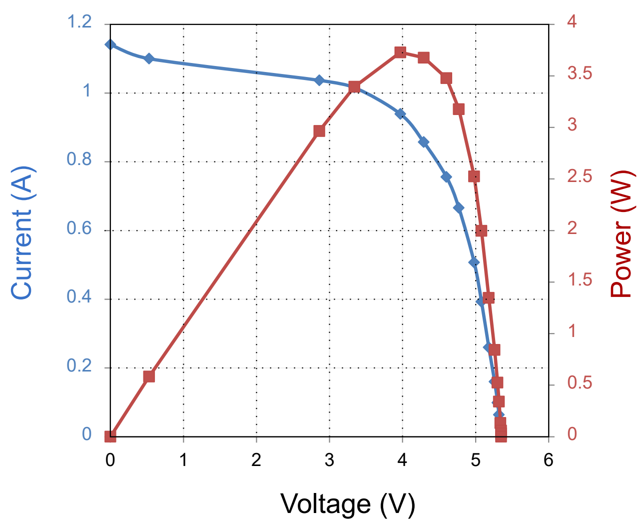

Figure 3: DC Characteristics of SP4.2-37 at 6150LUX

cannot produce a negative voltage. Hence, there is a DC part to every output of the panel. To accommodate this, a capacitor C_0 is added in series to the load resistor to create a high pass filter. This ensures the DC component of the signal is blocked. The final circuit is shown below in Fig. 4. Applying KVL on the circuit in Fig. 4, we get a transfer function as follows,

$$\left|\frac{v(\omega)}{i_{ph}(\omega)}\right|^2 = \left|\frac{\frac{R_{load}}{R_x}}{\frac{1}{r} + \frac{1}{R_x} + \frac{1}{R_{sh}} + j\omega C}\right|^2 \qquad (5)$$

Where,

$$R_x = R_s + \frac{1}{j\omega C} + R_{load}$$

We measured $v(\omega)$ with an oscilloscope. However, experimentally measuring $i_{ph}(\omega)$ might pose a problem as its value will be

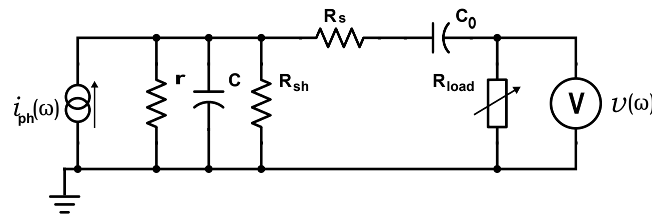

Figure 4: Equivalent Circuit model for AC signals

extremely small from the panels chosen. To measure this, we take the voltage $v(\omega)$ across a very small resistance. Then the AC peak to peak value is taken and divided by the resistance. We assume this to be approximately the right value because according to the DC characteristics of a PV panel, the current is constant over a large range of voltage, and is equal to I_{ph}. So, when a small resistance is kept as the load, the current is approximately equal to I_{ph}.

The results of the frequency response on the two panels are summarized in Table. 2. The operating frequency is selected based on how fast the comparator used in the next section, is able to respond to the changes in the input. The comparator demands a certain swing in voltage to exist in the input waveform to accurately produce the output. This value was selected as 200mV peak to peak. The responses are recorded in Fig. 5 and Fig. 6.

Table 2: Results obtained from the frequency response of the panels

Panel	CPC1824	SP4.2-37
r in Ω	213.00	623.62
C in nF	64	4.32
Preferable Bandwidth of operation in Hz	4700	15000

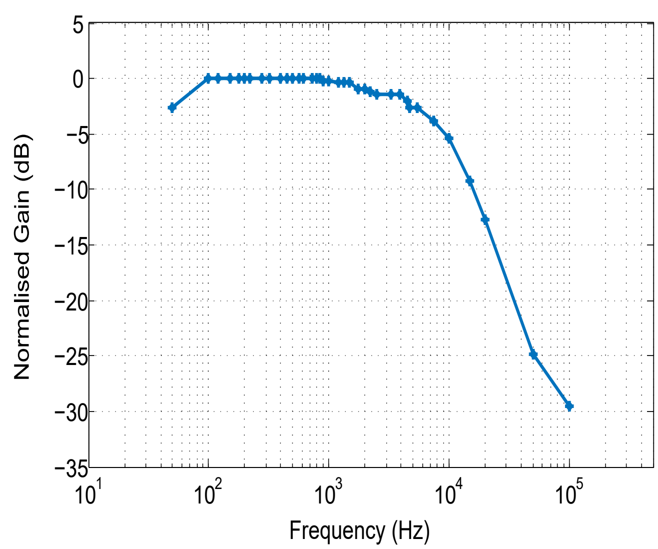

Figure 5: Frequency Response of CPC1824 for a C_0 value of $1\mu F$

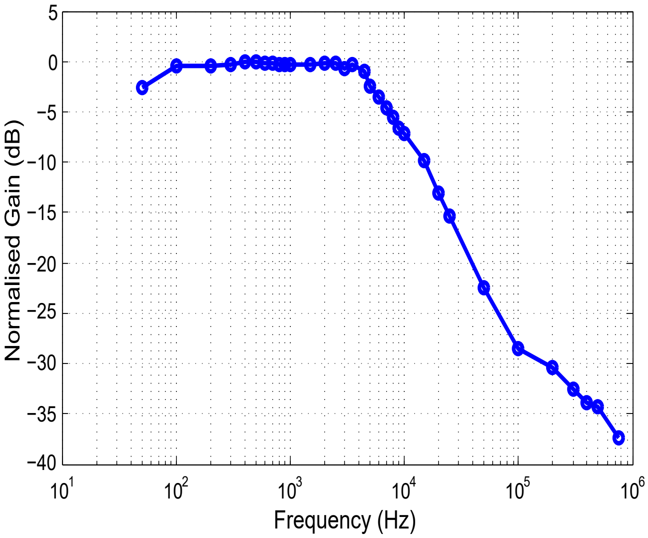

Figure 6: Frequency Response of SP4.2-37 for a C_0 value of $1\mu F$

The frequency response was found to be better for higher values of R_{load}. However, the 3-dB point retreats, resulting in a more 'peaky' response. Higher values of the capacitor C_0 means that the DC filtering efficiency is much better at lower frequencies. However, the response deteriorates at higher frequencies, making the panel unsuitable to work under higher frequencies [6].

3 DESIGN OF THE RECEIVER

The receiver we have designed is applicable for close-range embedded applications. This being said size was the primary criterion which we tried to satisfy. CPC1824 is 16 pin SOIC, which measures 10 mm x 6 mm. SP4.2-37 is a flexible amorphous silicon solar panel which measures 84 mm x 36.5 mm. For this reason, CPC1824 was used to design the panel, though SP4.2-37 shows a larger bandwidth. A distance of 21mm was maintained between the source and the panels for all our experiments. There were two main parts to the receiver design. (i) To extract the data accurately. The solar panel does not produce negative voltage like conventional antennae. This meant that we should be capable of handling the offset that was produced in the panel. (ii) To make this data readable by conventional systems, like microcontrollers. Due to the low power output of the panels, it was seen that the data was of a very low voltage and susceptible to noise. In order to abate these problems, we proposed a comparator design for the amplification.

3.1 Extraction of AC data

The input signal is given to a 1 W High Power LED using an arbitrary waveform generator (AWG 3021). The input signal is a square wave with peak-to-peak 8 V having a positive DC offset of 6 V. The values of the DC offset and peak-to-peak voltage are chosen because the solar panel can only produce positive voltage.

The source was implemented using OOK. For this reason, a square wave input was provided to the panel. However, the panel cannot produce a negative voltage, though it does follow the input

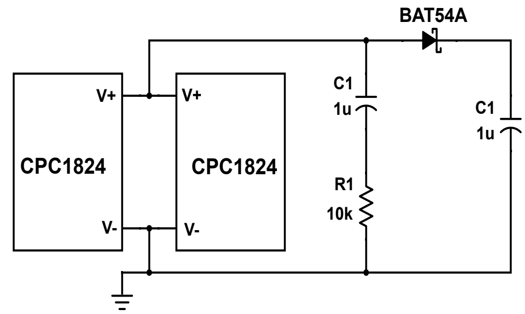

Figure 7: High pass filter and peak detector cascaded with the panels

that has a value greater than zero. For this purpose, a high pass filter was selected to extract the data accurately. The high pass filter uses a capacitor of 1 μF and a resistor of 10 kΩ. This gives a theoretical cutoff (3 dB) frequency of about 16 Hz. Hence, the DC component is effectively removed.

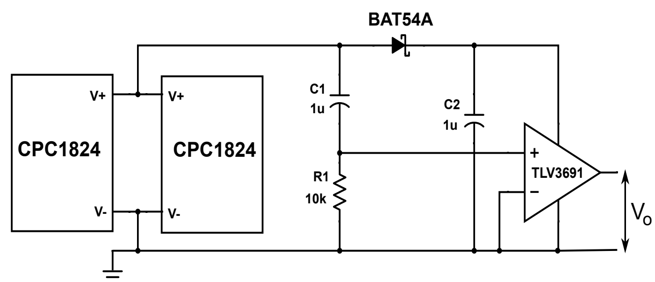

Figure 8: Receiver with the comparator connected

3.2 Amplification of Data and Energy Harvesting

The signal obtained from the high pass filter has a maximum peak to peak voltage of 120 mV. This is not sufficient to be read by any standard microcontrollers which require a minimum level of 1.8 V to 2 V to read the data. The signal has to be amplified. Our system aims to harvest energy from the incident intensity modulated light. A circuit is required to extract voltage from the output of the solar panel.

For the purpose of amplification of the data, we have used a nano-power comparator TLV 3691. The comparator operates with input supply voltage ranging from 0.9 V to 6.5 V. In order to power this comparator, we propose a peak detector circuit to harvest the peak voltage of the input waveform. This is more advantageous than extracting the dc part of the signal from the high pass filter as a peak detector will obtain more DC voltage. This paves a path for shorter bit lengths. For example, at a 20% duty cycle, the DC component of the OOK waveform is very less. This cannot power the comparator. However, a peak detector will yield a voltage 4 times greater. A schottky diode is used rather than a regular diode to reduce the voltage drop incurred. This further helps in harvesting maximum energy from the panels.

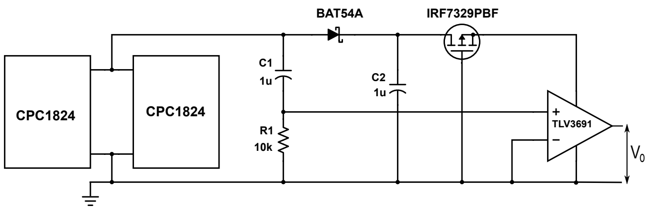

Figure 9: Final Design of the Receiver

The value of the capacitor used is 1 μF . For proper peak detection to take place we need to use a capacitor whose capacitance value is large enough that it does not discharge greatly during the down period(when the signal is consecutively low and the LED is turned off). A DC voltage of 4 V was obtained from the peak detector which can be used to provide energy to other loads. The combined circuit of the high pass filter and the peak detector is shown in Fig.7.

The circuit diagram with the connected comparator is shown in Fig. 8. Note that the positive rail of the comparator is connected to the output of the peak detector and the negative rail is connected to the circuit ground thus allowing the output to range from +4 V to 0 V.

3.3 Gating Circuit

One of the problems faced in the proposed approach above was that, due to the loading effect of the comparator the peak detector capacitor would not be charged at all. Most of the current was being drained by the comparator supply rail and the comparator was not being supplied enough voltage. It was required then to evolve a technique such that the comparator somehow was isolated from the rest of the circuit while the capacitor charges to the required level. This would prevent the comparator from draining all the current from the capacitor during periods of low power input. The solution proposed here is to use of gating circuits using MOSFETs. An added advantage provided by such a circuit is that its parasitic capacitance falls in parallel to the capacitor C_2. This increases the storage capacity of the harvesting circuit, thus allowing a greater length of 0s to be transmitted after charging. A series of designs were considered and we provide here the final implemented circuit shown in Fig. 9. A picture of the setup is shown in Fig. 10.

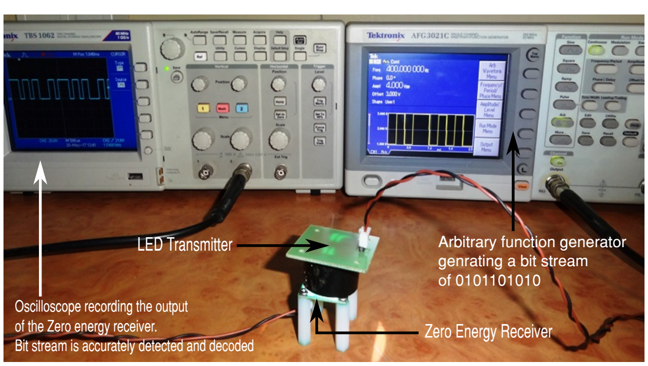

Figure 10: A view of the receiver decoding a random bit stream

4 EXPERIMENTS AND RESULTS

The square wave output from the comparator was obtained for a range of frequencies from 50 Hz to 3 kHz. Above 3 khz there was a high error in duty ratio until about 5 kHz where the comparator gave no input. This is a limitation of the selected comparator. It can only respond up to frequencies of about 5 kHz. This is a trade-off which had to be made considering the extremely small power consumption of the comparator. Further, the comparator introduces a constant delay of about 150μs between the input and the output. A set of simple experiments were conducted on the receiver and we report the following results through our exhaustive experiments.

4.1 Effect of incident wavelength on the Panel Response

To understand the effect of using light at different frequencies we tried to characterize the IV curve of the panel using different colour LEDs. The experiment was performed using LED of colours: White , Blue, Green and Red by giving the same input voltage to each of them individually. The results are as shown in Fig. 11. The current generated by the solar panel is proportional to the intensity of the incident light. The intensity of light directly depends on its wavelength. Blue which has the least wavelength generates the least current while red generates the greatest current for a single wavelength light.

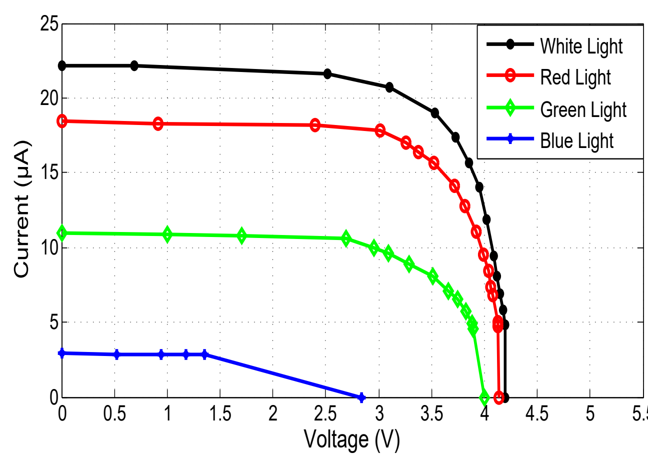

Figure 11: I-V Curves for different wavelengths of incident light

4.2 Necessary Bit Length

In order to estimate the minimum bit length necessary for transmission, bit error rate measures for various inputs were recorded. Observations were made over a period of 100 ms, 50 ms and 25 ms and a sequence of random bits was used to modulate the LED. Tektronix AFG3021C was used to generate this input stream. A dual channel oscilloscope TBS 1062 was used to obtain the data values. Fig. 12 shows a regressed curve obtained on measuring the bit error rate against bit length. Readings with error rates greater than 15% were ignored as 'unreadable' data streams. Moreover, it was found that when short stream of '0s'is between long streams of

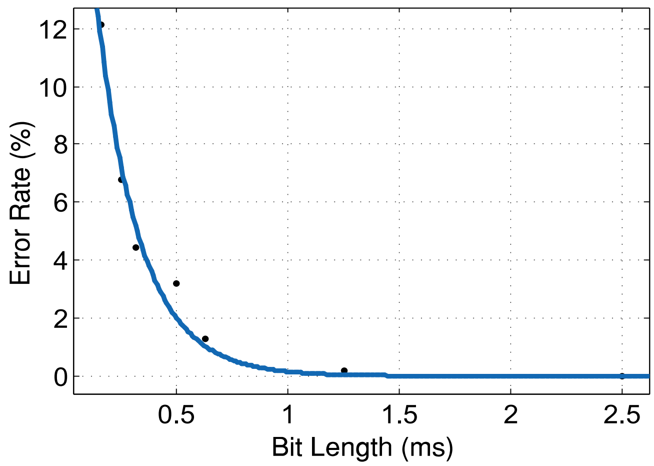

Figure 12: Bit error rate versus bit length

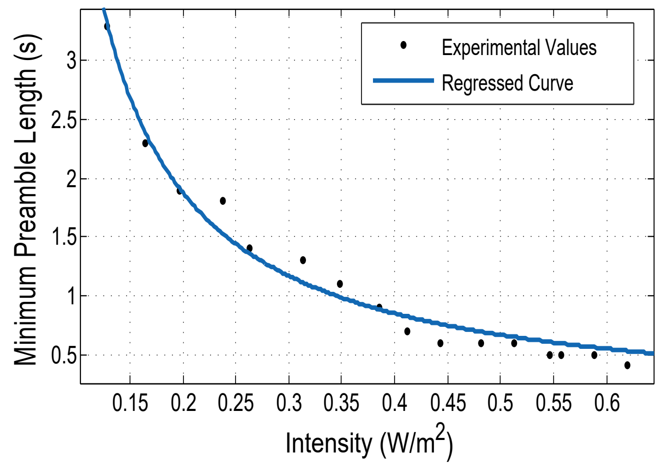

Figure 14: Dependence of preamble length on light intensity

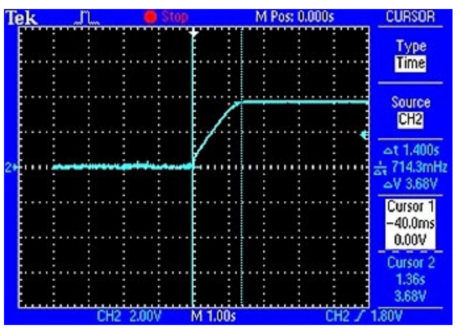

Figure 13: Charging time for a DC input. This dictates the preamble necessary at an input DC voltage of 3V, when the source and panel are apart by a distance of 21mm.

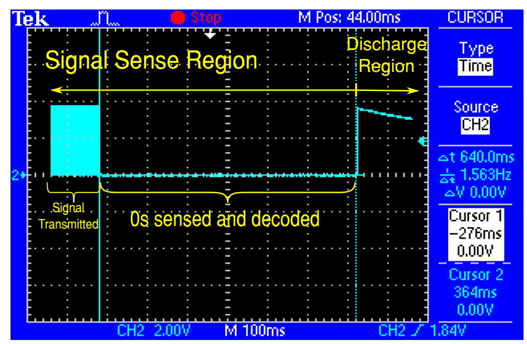

Figure 15: Response of the system when a continuous stream of 0s are transmitted. A maximum duration of 640ms can be tolerated by the system. This is independent of the bit length

'1s', then the 0 is not detected if the bit length is insufficient. For efficient reception, we infer that a minimum bit length of 0.625 ms is necessary.

4.3 Charging time before the comparator becomes operational

The peak detector capacitor cannot be instantaneously charged to its maximum value of 4 V. Thus before transmission of data a preamble consisting of only 1s must be sent for a period of time to charge the comparator. The amount of time required to charge was recorded for different frequencies of incident light. Experiments have shown that data for a period of 600 ms is rendered pointless if a DC preamble is not provided. A plot recording the charging time is shown in Fig. 13.

The panel was irradiated with white light of different intensities and the required preamble length was observed and plotted in Fig. 14. The result is as expected - more intensity would mean more current is generated and hence the charging of the capacitor would be faster.

4.4 Detecting a Continuous Stream of Zeroes

This experiment was conducted to estimate the longest duration for which the transmitter can be turned off while the comparator decodes it as a 0. Here, a sufficiently long preamble was provided followed by a square wave of a set frequency. The LED was then turned off and the duration for which the output is 0 was recorded in the oscilloscope. After a duration of 640ms, the capacitor undergoes discharge, as shown in Fig. 15. This duration was invariant to the input bit length of data. The cold start for the zero energy receiver was evaluated to be about 1.4s in subsection *C*. Since the energy in the capacitor can sustain for 640ms before a discharge, we evaluated the time required to revert to full charge to about 300ms. This system has the ability to handle several input bit patterns including 0s for about 640ms. Furthermore, if the supported bit rate is enhanced, then the system would offer improved data input pattern versatility.

Further, the source bit sequence could be scrambled so that the bit consecutive '0 bits are reduced.

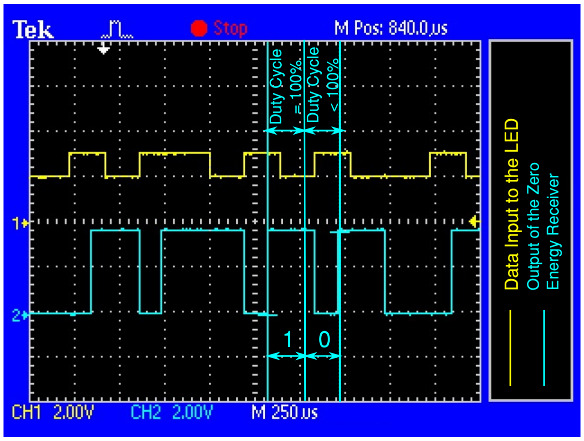

Figure 16: Duty Cycle approach to decode high date rates

4.5 Improving the Data Rate

In the results obtained in subsection B of this section, it can be inferred that there exists a trade-off between the data rate and the accuracy of decoding. In this subsection, we propose a method that can be implemented so as to increase data rates while ensuring a high decoding accuracy. This method exploits the parasitics of the solar panel. To demonstrate this feature, a bit stream of 0101101010 was transmitted with a bit length of 0.20ms.

It is seen from Fig. 16 that the length of the decoded 1 bit is longer than 0.20ms while the length of the 0 bit is of a shorter duration, especially when it is sandwiched between 1s. In order to accurately obtain the data, a duty cycle approach can be conducted. Since the bit length is specified, the duty cycle of the pulse for the duration of bit can be observed. If the value is 100%, then a 1 is read. For any value below 100%, a 0 is read. Using this method, the receiver can process data rates from 2.5 to 10 kbps.

The work presented in this article provides a proof of concept of harvest-detect decode simultaneously.

5 CONCLUSION

In the context of Internet of Things (IoT), VLC has unique position such as privacy and security with respect to the intended recipients of a transmission. With miniaturization, the energy requirement has also been one of the important aspects of IoT devices. This work explores VLC based system that also harvests the energy while the transmission is ongoing. We demonstrated such a system through implementation. We proposed VLC receiver circuit that is implemented with great success in indoor environments. It is observed that as long as ambient light whose intensity is not far greater than the switching LED intensity, the receiver can operate without discrepancy. Hence, the receiver is useful close range optical wireless communications. Almost any LED can be modulated to transmit the data. This is an exciting prospect for the proposed receiver system. One of the compelling features of this receiver is its non-requirement for an external energy source. Coupled with the extremely small size of the components, the receiver is highly portable and can be used in a wide variety of applications, being able to support data rates as high as 10kbps.

REFERENCES

[1] Sukhvir Singh, Gholamreza Kakamanshadi, and Savita Gupta. 2015. *Visible Light Communication-An Emerging Wireless Communication Technology* Proceedings of 2015 RAECS UIET Panjab University Chandigarh, December 2015..

[2] Jacqueline J.George, Mohammed Hayder Mustafa, Nada Mahjoub Osman, Nuha Hashim Ahmed and DaâĂŹad Mohammed Hamed. 2014. *A Survey on Visible Light Communication* IJECS, Volume 3, Issue 2, February 2014..

[3] Saadi M, Wattisuttikulkij L, Zhao Y and Sangwongngam P. 2013. *Visible Light Communication: Opportunities, Challenges and Channel Models* IJEI, Volume 2, No 1, 2013..

[4] Shinichiro Haruyama 2013. *Visible Light Communication using Sustainable LED Lights* Proceedings of ITU Kaleidoscope: Building Sustainable Communities, Kyoto, 2013, pp. 1-6..

[5] Green M. A. . *High Efficiency Solar Cells*. Springer Publications

[6] Zixiong Wang, Dobroslav Tsonev, Stefan Videv, and Harald Haas 2015. *On the Design of a Solar-Panel Receiver for Optical Wireless Communications with Simultaneous Energy Harvesting* IEEE Journal on selected areas in communication, Vol. 33, August 2015..

[7] Sung-Man Kim and Ji-San Won 2013. *Simultaneous Reception of Visible Light Communication and Optical Energy using a Solar Cell Receiver* 2013 International Conference on ICT Convergence (ICTC), Jeju, 2013, pp. 896-897..

[8] Joyce Sariol Ramos, Ilker Demirkol, Josep Paradells, Daniel VÃűssing, Karim M. Gad and Martin Kasemann 2016. *Towards Energy-Autonomous Wake-up Receiver using Visible Light Communication* 2016 13th IEEE Annual Consumer Communications & Networking Conference (CCNC).

[9] Xiaozhe Fan, Walter D. Leon-Salas and Thomas Fischer 2016. *An LED-Based Image Sensor with Energy Harvesting and Projection Capabilities* SENSORS, 2016 IEEE.

[10] Bilal Malik and Xun Zhang 2015. *Solar Panel Receiver System Implementation for Visible Light Communication* 2015 IEEE International Conference on Electronics, Circuits, and Systems (ICECS).

[11] Marcelo Gradella Villalva, Jonas Rafael Gazoli, and Ernesto Ruppert Filho 2009. *Comprehensive Approach to Modeling and Simulation of Photovoltaic Arrays* IEEE Transactions on Power Electronics, May 2009..

[12] Rauschenbach H. S. 1980. *Solar Cell Array Design Handbook* NewYork: Van Nostrand Reinhold, 1980..

[13] Appelbaum J. and Peled A. 2013. *Parameters extraction of solar cells âĂŞ A comparative examination of three methods* Solar Energy Materials & Solar Cells, 2013..

[14] Huan-Liang Tsai, Ci-Siang Tu and Yi-Jie Su 2008. *Development of Generalized Photovoltaic Model Using MATLAB/SIMULINK* Proceedings of the World Congress on Engineering and Computer Science 2008 WCECS 2008, October 22 - 24, 2008, San Francisco, USA.

[15] Jamadagni H S, Varun Gowtham, Soumya N S and Prabhakar T V 2014. *A Novel and Scalable LED Communication System* 2014 Sixth International Conference on Communication Systems and Networks (COMSNETS), Bangalore, 2014, pp. 1-3..